Supplementary Data

Supplementary Data comprises 4 Supplementary Figures, 4 Supplementary Movies, 2 Supplementary Tables and Additional References.

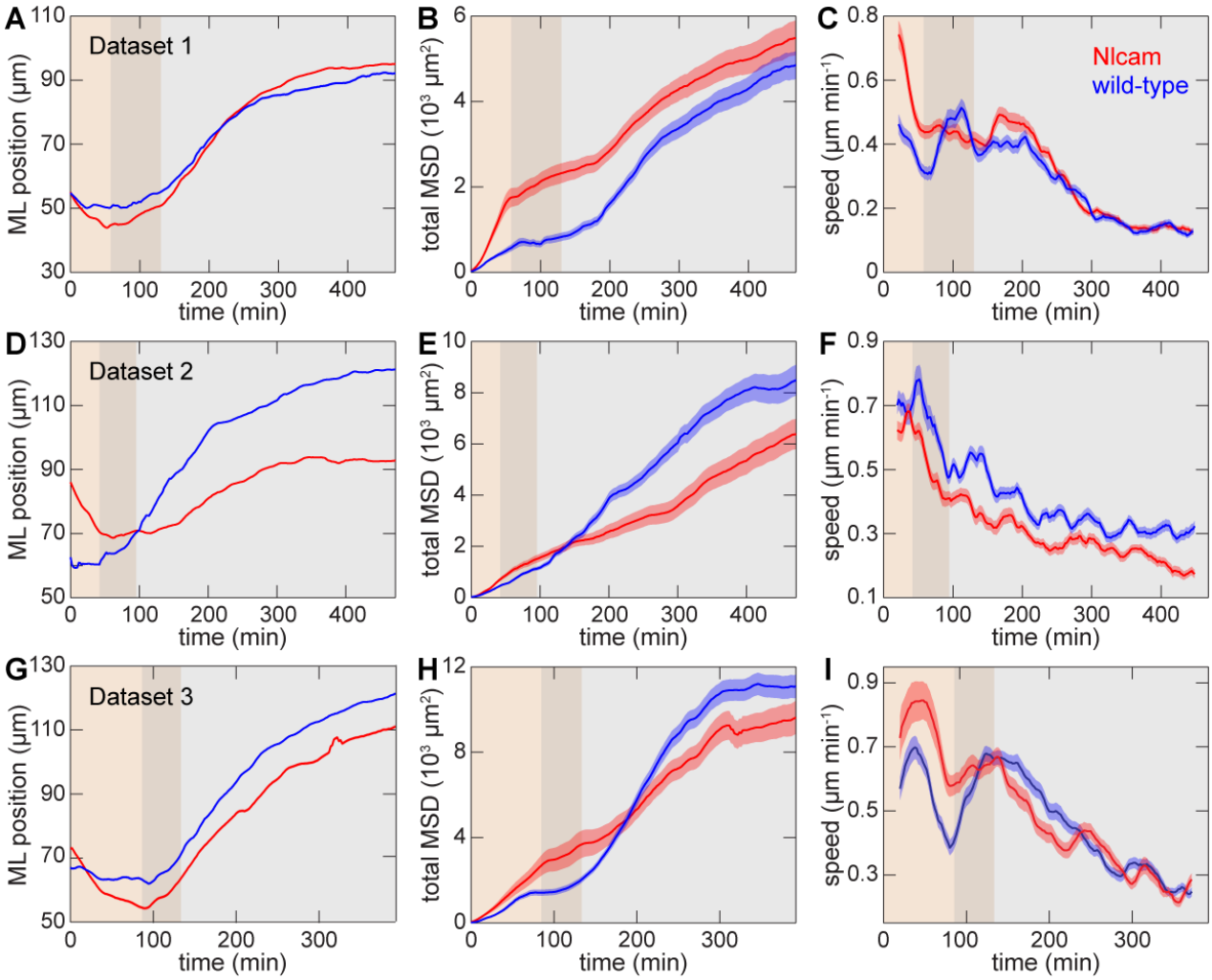

Supplementary Figure 1: Global statistical analysis of cell behaviour

Selected global statistics for the wt and *nlcam*$^{+}$ tracked eye-field cells for three datasets. A, D, G: ML position. B, E, H: Total MSD. C, F, I: Speed (averaged over 20 time points (~40 minutes)). Only minor differences are visible between the two populations.

In this and subsequent figures, blue = wt cells; red = *nlcam*$^{+}$ cells. Paler shading indicates the standard error. Overlapping boxes show the approximate periods of convergence (brown) and evagination (grey).

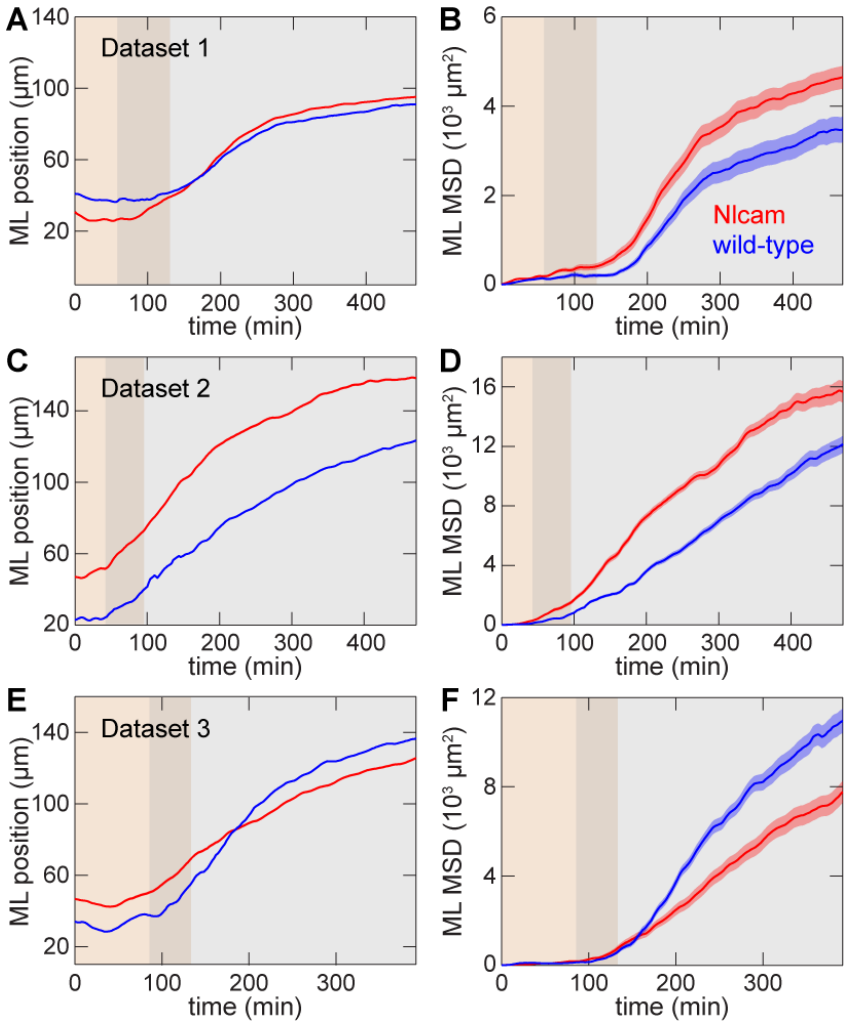

Supplementary Figure 2: Statistical analysis of migratory dynamics of medial retinal cells

Graphs show selected statistics for the medial groups of cells only, for three datasets. A, C, E: ML position. B, D, F: MSD in the ML axis. No consistent differences between wt and *nlcam*$^{+}$ populations can be seen.

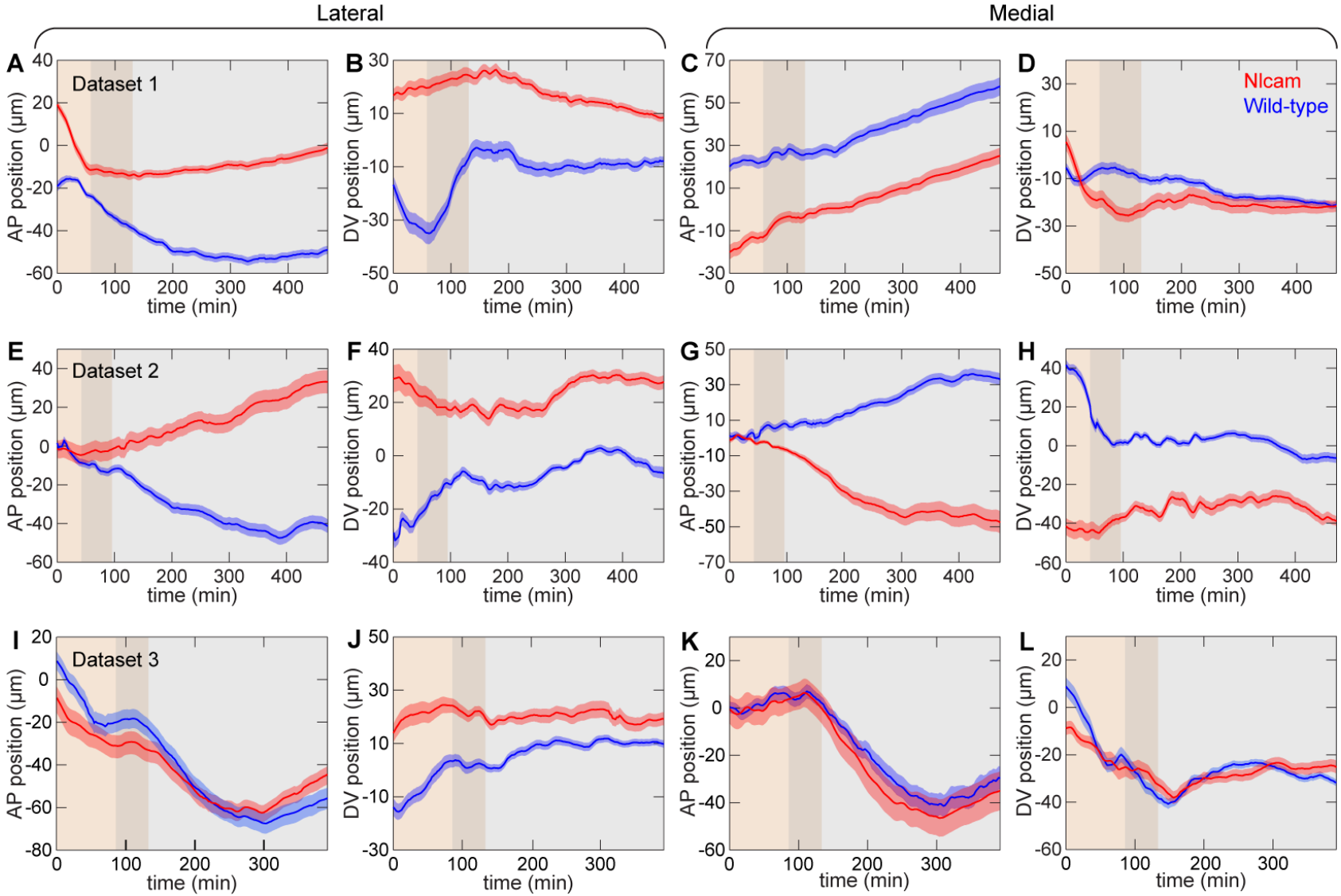
Lateral
Medial
A
Dataset 1
B
C
D
Nlcam
Wild-type
E
Dataset 2
F
G
H
I
Dataset 3
J
K
L
AP position (μm)
DV position (μm)
time (min)

Supplementary Figure 3: Distribution of wt and *nlcam*$^{+}$ cells in the antero-posterior and dorso-ventral axes

Graphs show positions of lateral (A, B, E, F, I, J) and medial (C, D, G, H, K, L) cells in the AP (A, C, E, G, I, K) and DV (B, D, F, H, J, L) axes, for three datasets. There is a consistent bias for lateral *nlcam*$^{+}$ cells to be more dorsally located than their wt counterparts (B, F, J). No consistent distribution is seen for the lateral cells in the AP axis, or for medial cells in either axis.

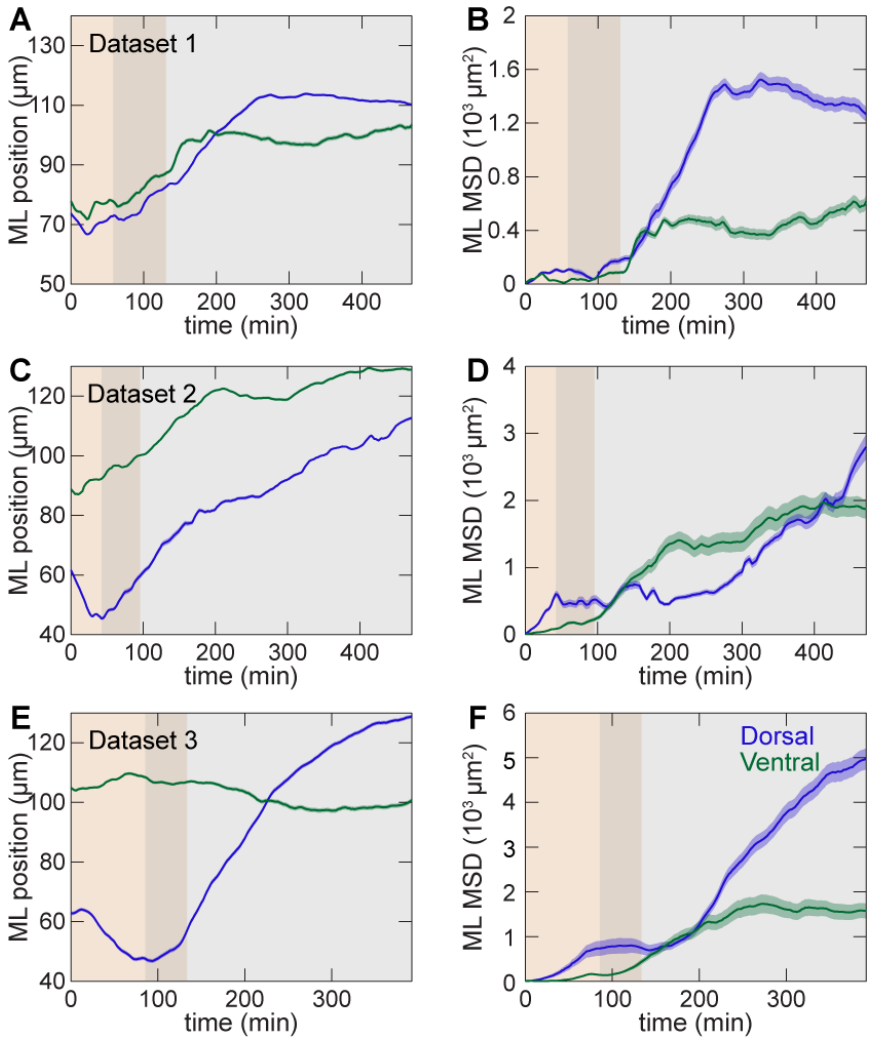

Supplementary Figure 4: Analysis of the effects of dorso-ventral position on cell migration

The lateral wt cells for each dataset were split into dorsal and ventral groups. Statistics show the behaviour of dorsal versus ventral wt cells. Blue: dorsal wt cells. Green: ventral wt cells. While dorsal cells clearly migrate further in towards the midline A, C, E), similar to *nlcam*$^{+}$ cells, they do so with very different dynamics, as revealed by the ML MSD (B, D, F).

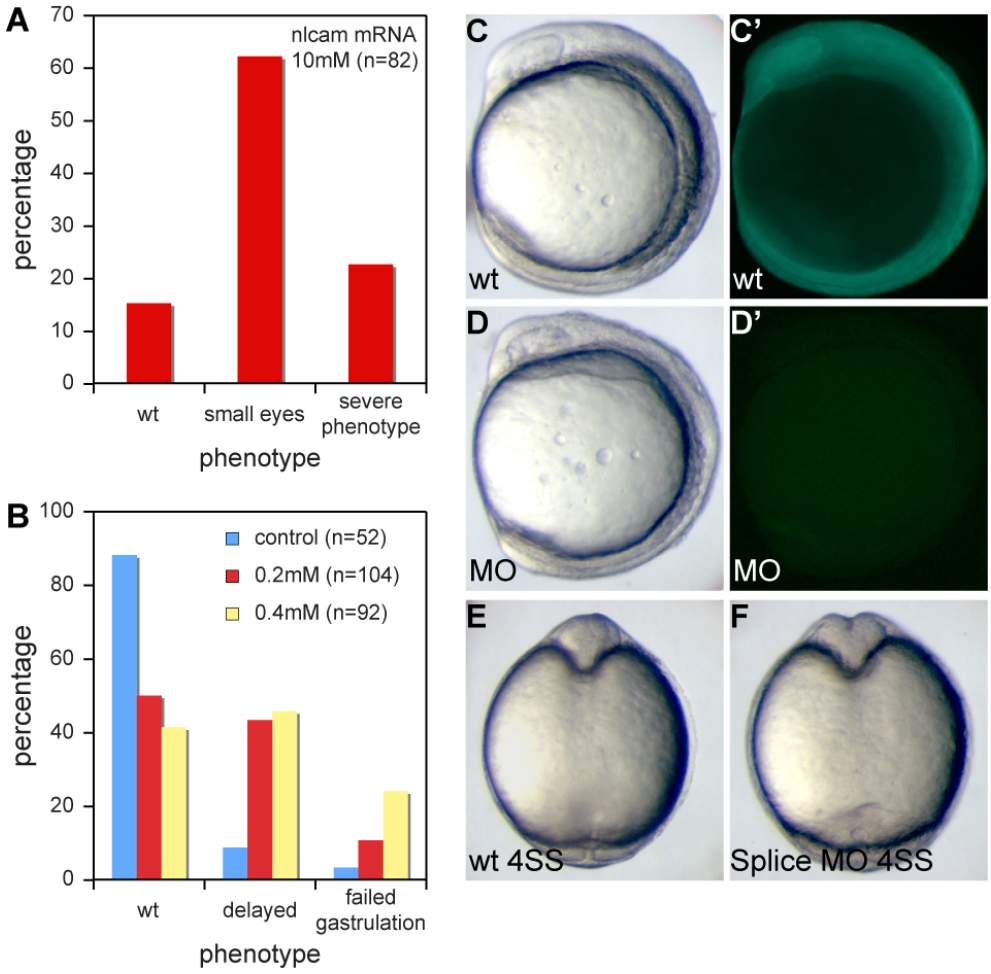

Supplementary Figure 5: Quantification and controls for *nlcam* over-expression and morpholino

A: Quantification of the frequency of phenotypes observed upon injection of *nlcam* mRNA at 10ng/μl. Results show one representative experiment (ie embryos from a single batch injected at the same time). “Severe phenotype” denotes failed or disrupted gastrulation, or severe convergent-extension and/or neural tube defects.

B: Quantification of the frequency of phenotypes observed upon injection of *nlcam* ATG morpholino at either 0.2mM or 0.4mM (as indicated). As above, results show one representative experiment.

C, D: *nlcam* ATG morpholino represses GFP expression from a construct in which the target sequence is placed upstream of the GFP coding sequence. In embryos co-injected with this construct plus the morpholino, no GFP expression can be seen.

E, F: A second morpholino, targeted against the e3, i4 splice junction, phenocopes the ATG morpholino.

Supplementary Figure 6: Putative Rx3 binding sites in the promoter regions of other vertebrate *nlcam* orthologs

Rx binding sites in the upstream regions of *alcam* in frog, chicken and human (positions -5986, -6281, -3867 before the transcription start site respectively). The nucleotides matching perfectly the core Rx consensus binding sequence have been highlighted in bold.

Supplementary Movie S1: Live imaging of cell migration during optic vesicle morphogenesis

Maximum projection (dorsal view) of confocal data from Dataset 1, showing RPC migration during the period of optic vesicle morphogenesis. Z-stacks were taken approximately every 2 minutes, for a total of 8 hours, of which the first 7 are shown here.
The eye field is labelled with Rx3::GFP; transplanted wt cells are marked by eBFP2-Nuc, and transplanted *nlcam*$^{+}$ cells by H2B-mRFP. The raw data has been corrected for changes in GFP intensity, photobleaching, drift and rotation.

Supplementary Movie S2: Reconstruction of cell movements

Movie shows a rendered reconstruction of the segmented and tracked data from Dataset 1. Wt nuclei are shown in cyan; *nlcam*$^{+}$ nuclei in red. The tracked RPCs are shown in brighter colours; dimmer colours indicate untracked RPCs or non-retinal cells. Yellow spots indicate tracked wt telencephalic nuclei. Trails behind spots indicate nuclear positions over the previous 10 timepoints.

Supplementary Movie S3: Tracking of RPCs reveals differential migration of wt and *nlcam*$^{+}$ cells

Rendered reconstruction of those RPCs that can be tracked throughout the recording, showing dorsal, frontal and lateral views. *nlcam*$^{+}$ cells occupy more dorsal positions at the onset of recording. During the initial phase of convergence (covering approximately the first hour), laterally located *nlcam*$^{+}$ cells migrate further towards the midline than do equivalent wt cells. Subsequently, all cells migrate out into the optic vesicles. However, wt cells occupy more lateral positions than do *nlcam*$^{+}$ cells.

Supplementary Movie S4: Vectorial representation of cell movements

Movie shows vectorial representation of Dataset 1. The length and direction of arrows indicates the position of each nucleus after 10 timepoints. Longer arrows therefore represent greater displacement. The data is collapsed in the dorso-ventral axis for simplicity. Cyan: lateral wt RPCs; blue: medial wt RPCs; red: lateral *nlcam*$^{+}$ RPCs; orange: medial *nlcam*$^{+}$ RPCs. The long red arrows at the beginning of the movie indicate the rapid midline-directed migration of *nlcam*$^{+}$ cells.

Supplementary Table 1: In situ analysis of CAM expression in the anterior neural plate

Gene	ENSEMBL ID	Expression pattern at 6SS	Changed in *rx3/chk*	Reference
Cdh1	ENSDARG00000024371	Anterior mesendoderm (polster)	No	(Babb et al., 2001)
Cdh2	ENSDARG00000018693	Ubiquitous	No	(Bitzur et al., 1994)
Ncam1	ENSDARG00000056181	Anterior CNS	No	(Mizuno et al., 2001)
Ncam2	ENSDARG00000017466	Not expressed	No	(Mizuno et al., 2001)
Ncam3	ENSDARG00000007220	Bilateral stripes in neural tube	No	(Mizuno et al., 2001)
Mcam	ENSDARG00000005368	Medoderm, tailbud	No	(Kudoh et al., 2001)
Bcam	ENSDARG00000070367	Anterior neural plate, notochord	No	(Thisse et al., 2008)
Alcam	ENSDARG00000026531	Lateral mesoderm, anterior somites	No	(Mann et al., 2006)
Nlcam	ENSDARG00000058538	Dorsal forebrain, MHB, trunk neural tube	Yes	(Mann et al., 2006)
Itgb1b	ENSDARG00000053255	Not expressed	No	(Thisse et al., 2001)
Itgb4	ENSDARG00000028507	Not expressed	No	N/A
Itgb5	ENSDARG00000012942	Tailbud: Kupffer's vesicle	No	(Ablooglu et al., 2007)

Summary of the genes tested and their endogenous expression pattern at 6SS. Only *nlcam* showed a significantly altered expression pattern in *chk* mutants compared to wt.

Supplementary Table 2: Key statistical parameters of different wt and *nlcam*$^+$ cell populations during convergence

		Initial DV position (μm)	Distance converged (μm)	MSD accumulated (μm^2)	% of final MSD
Dataset 1	Lateral wt	0 ± 5.7	1.7 ± 0.4	47.8 ± 13.4	5.1
	Dorso-lateral wt	30.6 ± 1.8	2.3 ± 1.1	87.9 ± 23.8	7.0
	Lateral *nlcam*$^+$	31.7 ± 3.4	18.4 ± 0.4	939.1 ± 207.2	62.0
	Telencephalic wt	14.6 ± 14.5	25.5 ±5.0	824.8 ±266.5	11.6
Dataset 2	Lateral wt	0 ± 3.5	4.3 ± 0.2	226.2 ± 35.8	15.8
	Dorso-lateral wt	55.0 ± 12.5	13.8 ± 2.8	439.1 ± 241.1	15.5
	Lateral *nlcam*$^+$	59.2 ± 9.2	18.5 ± 0.7	924.6 ± 160.0	88.0
	Telencephalic wt	13.9 ± 13.5	34.5 ± 3.8	1418.0 ± 339.4	16.5
Dataset 3	Lateral wt	0 ± 4.0	4.8 ± 0.6	226.5 ± 73.3	6.6
	Dorso-lateral wt	25.6 ± 2.4	11.6 ± 0.6	386.8 ± 133.9	7.7
	Lateral *nlcam*$^+$	25.9 ± 4.3	21.8 ± 1.0	1300.7 ± 396.2	51.4
	Telencephalic wt	-8.1 ± 14.4	27.6 ± 4.5	1045.0 ± 391.8	10.3

Table shows key parameters for lateral wt, dorso-lateral wt, lateral *nlcam*$^+$ and wt telencephalic groups for each dataset. Initial DV position (relative to the mean of the lateral wt group), distance converged and MSD accumulated over the first 60min of recording are given as mean ± standard error. Additionally, the percentage of final MSD reached during the first hour of recording is shown. The differences between wt and *nlcam*$^+$ RPCs are most clearly exemplified by these MSD parameters. These reveal the similarity between *nlcam*$^+$ RPCs and telencephalic cells, which accumulate similar MSD during this initial convergence phase. Important similarities are shown highlighted in red; differences in blue.

References

Ablooglu, A. J., Kang, J., Handin, R. I., Traver, D., and Shattil, S. J. (2007). The zebrafish vitronectin receptor: characterization of integrin alphaV and beta3 expression patterns in early vertebrate development. *Dev Dyn* **236,** 2268-76.

Babb, S. G., Barnett, J., Doedens, A. L., Cobb, N., Liu, Q., Sorkin, B. C., Yelick, P. C., Raymond, P. A., and Marrs, J. A. (2001). Zebrafish E-cadherin: expression during early embryogenesis and regulation during brain development. *Dev Dyn* **221,** 231-7.

Bitzur, S., Kam, Z., and Geiger, B. (1994). Structure and distribution of N-cadherin in developing zebrafish embryos: morphogenetic effects of ectopic over-expression. *Dev Dyn* **201,** 121-36.

Kudoh, T., Tsang, M., Hukriede, N.A., Chen, X., Dedekian, M., Clarke, C.J., Kiang, A., Schultz, S., Epstein, J.A., Toyama, R., and Dawid, I.B. (2001) A gene expression screen in zebrafish embryogenesis. ZFIN Direct Data Submission (http://zfin.org).

Mann, C., Hinits, Y., and Hughes, S. (2006). Comparison of neurolin (ALCAM) and neurolin-like cell adhesion molecule (NLCAM) expression in zebrafish. *Gene Expression Patterns*.

Mizuno, T., Kawasaki, M., Nakahira, M., Kagamiyama, H., Kikuchi, Y., Okamoto, H., Mori, K., and Yoshihara, Y. (2001). Molecular diversity in zebrafish NCAM family: three members with different VASE usage and distinct localization. *Mol Cell Neurosci* **18,** 119-30.

Thisse, B., Wright, G.J., Thisse, C. (2008) Embryonic and Larval Expression Patterns from a Large Scale Screening for Novel Low Affinity Extracelular Protein Interactions. ZFIN Direct Data Submission (http://zfin.org).